Electrochemical Quartz Crystal Microbalance Study of Tetracyanoquinodimethane Conducting Salt Electrodes

C. Donald Evans and James Q. Chambers*

Department of Chemistry, University of Tennessee, Knoxville, Tennessee 37996

Received November 1, 1993. Revised Manuscript Received February 8, 1994®

Electrochemical quartz crystal microgravimetry (EQCM) has been employed to study tetracyanoquinodimethane (TCNQ) redox chemistry in concentrated aqueous electrolytes. Surface films of the TCNQ were generated by oxidation of solid crystallite films of 9-aminoacridinium $(TCNQ)_2$ on gold EQCM substrates in contact with 1 M $Ca(OAc)_2$ or 1 M KOAc. After redox cycling between the neutral TCNQ and $TCNQ^-/(TCNQ_2)^{2-}$ states, the EQCM frequency transients were consistent with permselective ion motion for the cathodic insertion and anodic expulsion of $CaOAc^+$ and $K(H_2O)_4^+$ into and out of the solid-state lattice. The initial reduction step after electrogeneration of the TCNQ surface state gave anomalously large frequency transients indicative of extensive hydration or surface structural change. Chronoamperometric EQCM experiments at low overpotentials gave insight into the coupling of electron and ion motion during the TCNQ redox process. The anodic frequency transients indicated a two-step process: (i) insertion of anions of the supporting electrolyte in order to maintain charge neutrality; (ii) followed by slow diffusional loss of neutral electrolyte from the TCNQ solid-state lattice. This process gave rise to significant frequency transients in the EQCM cyclic voltammetry experiments at potentials where there was essentially no faradaic reaction taking place.

Electrically conducting organic salts in the TTF–TCNQ family are members of a novel class of donor–acceptor compounds, in which charge-transfer partners interact to produce charge-delocalized structures of low dimensionality. The intriguing solid-state properties of these materials have been extensively researched due to their metallic nature. Now 20 years after the reports of the high conductivity of the TTF–TCNQ prototypal material,[1,2] the set of compounds known to display electronic conductivity in the solid state has been expanded considerably to include a variety of organic and organometallic partners.[3]

The solution electrochemical behavior of these materials, i.e., the nature of charge transport at the organic metal/electrolyte solution interface, has been less well studied. The pioneering work of Jaeger and Bard on the TTF–TCNQ electrodes showed that lattice redox reactions could be activated for these materials when they were in contact with electrolyte solutions where the donor and acceptor salts of the electrolyte ions were insoluble.[4] Under voltammetric conditions, lattice redox processes took place that corresponded to incorporation or release of hundreds of equivalent monolayers of counterions into or out of the electrode lattice:

$$\text{donor site} + yX^- \xrightarrow{\text{oxid}} [\text{donor site}]X_y$$

$$\text{acceptor site} + zM^+ \xrightarrow{\text{redn}} [\text{acceptor site}]M_z \qquad (1)$$

Typically, while the above processes are electrochemically irreversible, exhibiting large peak separations, chemical reversibility is often observed upon repeated potential cycling. Others have reported on the voltammetric behavior of conducting organic salt electrodes,[5,6] and Ward has provided a comprehensive review on the subject.[3]

The electrochemical quartz crystal microbalance (EQCM) technique has been established as a powerful in situ method that permits mass and/or viscoelastic changes at the solid/solution interface to be monitored.[7,8] This technique has been used to study a variety of phenomena including the mass changes during redox cycling of conducting salt electrodes. Of recent interest is the analytical methodology of Hillman and Bruckenstein that allows differentiation between rate-limiting processes due to the motion of electrons, neutral or charged species during the EQCM experiment as well as the demonstration of the existence of global equilibrium.[9] These researchers and their colleagues have applied their general approach with success to analysis of the electrochemical "doping" of conducting polymer films of the poly(thiophene) and poly(pyrrole) genre.[10]

Extraction of precise estimates of mass changes from EQCM data is made difficult by several experimental artifacts.[7,8] First, the Sauerbrey equation applies only to thin uniform rigid films in contact with the quartz crystal surface. Frequency changes will also be detected when the viscoelastic properties of the film/solution interface are altered. For the organic salt interface with aqueous electrolytes, it is difficult to separate changes in the latter

® Abstract published in *Advance ACS Abstracts*, March 15, 1994.

(1) Ferraris, J.; Cowan, D. O.; Walatka, V.; Perlstein, J. H. *J. Am. Chem. Soc.* **1973**, *95*, 948.
(2) Ehrenfreund, E.; Rybaczewski, E. F.; Garito, A. F.; Heeger, A. J. *Phys. Rev. Lett.* **1972**, *28*, 873.
(3) Ward, M. D. In *Electroanalytical Chemistry*; Bard, A. J., Ed.; Marcel Dekker: New York, 1989; Vol. 16.
(4) Jaeger, C. D.; Bard, A. J. *J. Am. Chem. Soc.* **1979**, *101*, 4840; **1980**, *102*, 5435.
(5) Freund, M. S.; Brajter-Toth, A.; Ward, M. D. *J. Electroanal. Chem.* **1990**, *289*, 127.
(6) Zhao, S.; Korell, U.; Cuccia, L.; Lennox, R. B. *J. Phys. Chem.* **1992**, *96*, 5641.
(7) Buttry, D. A. In *Electroanalytical Chemistry*; Bard, A. J., Ed.; Marcel Dekker: New York, 1991; Vol. 17.
(8) Buttry, D. A.; Ward, M. D. *Chem. Rev.* **1992**, *92*, 1355–1379.

0897-4756/94/2806-0454$04.50/0

from mass changes due to motion of species in and out of an amorphous electrode phase. Second there is a well-known and significant radial dependence of the response function of a quartz crystal microbalance. This dependency makes calibration procedures based on electrodeposition of metal such as silver or copper nonquantitative when applied to nonuniform films. Since the procedure used to lay down the TCNQ films of this study did not produce uniform coverage of the electrode surface, the EQCM data allow only qualitative conclusions to be reached. However, relative values of the frequency changes obtained as a given surface film is redox cycled do give mechanistic insight on the nature of the conducting salt electrode reactions.

Previously, we have reported on the spectroelectrochemistry of the TCNQ redox couple that is generated by electrooxidation of films of a 9-aminoacridinium salt on solid electrodes.[11] The redox reactions of the resulting surface film were identified with a neutral/(dimer dianion) TCNQ couple in concentrated K^+(aq) electrolyte solutions. This redox chemistry is in accord with previous studies either of TCNQ in aqueous solutions[12,13] or of TCNQ polymer films in contact with aqueous solution.[14] Charge neutrality in the surface film redox reactions was presumably maintained by lattice intercalation of potassium ions in the manner of eq 1 above. To understand the redox process more fully, we have now carried out an EQCM study on the (9-aminoacridinium)$(TCNQ)_2$ electrodes. Both cyclic voltammetry and chronoamperometry were used to elucidate the asymmetric nature of the lattice reduction and oxidation steps of the TCNQ couple in this system.

Experimental Section

Materials. The 9-aminoacridinium TCNQ salt, 9-AA^+-$(TCNQ)_2^-$, was synthesized as described previously.[11] The supporting electrolytes, which were reagent grade, were used without further purification.

Instrumentation. The 5-MHz AT-cut planoconvex quartz crystals used in this study were supplied by ICM Corp of Oklahoma City. They were supplied with 6.8-mm-diameter vapor deposited Au electrodes (area = 0.363 cm^2). The QCM crystal was sealed to a tubular glass stub with epoxy cement to form the electrochemical cell. The stub diameter was greater than the active area of the crystal. An oscillator circuit operating in the feedback mode and supplied by a 9-V power supply was used to drive the QCM crystal at its resonance frequency. The frequency was measured with a Keithley 775A frequency counter using a gating time of 50 ms. The working electrode contact of the QCM crystal was maintained at the true ground of the oscillator circuit. The potentiostat for the EQCM experiments consisted of a simple operational amplifier circuit with a sweep generator input. The current signal was measured across a feedback resistor using a Keithley 196 digital voltmeter. Data acquisition was performed via an IEEE 488 interface bus and an AT PC.

The EQCM cell held ca. 5 mL of solution. A Pt spiral served as the counter electrode and the reference electrode was a commercial S.C.E. Cyclic voltammetry not associated with EQCM measurements was performed with a BAS-100 electrochemical analyzer.

Procedures. The 9-$AA^+(TCNQ)_2^-$ film was applied to the working electrode with a cotton swab as described previously.[11] It was necessary to use unpolished electrodes in order to maintain an adherent film. Care was taken to cover the electrode surface as completely as possible. The film thickness could be estimated from the frequency difference between the bare surface and the coated surface in air using the relation $d_f = d_Q(\Delta f/f_0)$, where d_Q is the thickness of the AT-cut quartz crystal. Typical values were on the order of 0.1 μm. The electrolyte solution was then slowly added to the cell such that a maximum depth of 2 cm rested on the quartz crystal. The film was activated either by application of a potential of 600 mV followed by a voltage sweep to −100 mV or by an initial sweep from 0 to 600 mV. After the initial activation, the film was then cycled between potentials that encompassed the TCNQ redox processes as described previously. Frequency and current data pairs were collected during both the activation and the redox cycling steps.

For the EQCM chronoamperometric experiments, the films were activated using a BAS-100 potentiostat until a well-behaved TCNQ redox couple was observed. Then combined EQCM frequency-current data were collected when the film was stepped from a fully oxidized or reduced state to a potential on the rising segment of the voltammetric reduction or oxidation wave, respectively. When the applied potential was restricted to the foot of the voltammetric peaks, the observed transients were compatible with the sampling frequency and the gating time of the counter.

The EQCM crystals were cleaned for reuse by rinsing with water, followed by sonication in acetone and a final wash with ethanol. The surfaces were then allowed to air dry. We found that the gold electrode contacts on the crystals as supplied by the manufacturer had a finite lifetime due to loss of contact sufficient to carry the electrochemical currents. Thus the data reported in this paper were obtained on surfaces that had been recoated with conducting salts no more than three times.

The QCM was calibrated by constant current deposition of silver from a 0.5 M HNO_3, 0.5 M $AgNO_3$ solution. A calibration factor, C_f, of 300 ± 49 Hz/μg was obtained.

A radial dependency of the mass sensitivity was observed in these experiments as expected based on literature reports.[15,16] A coating of 9-$AA^+(TCNQ)_2^-$ applied to the center of the gold contact to the quartz crystal resulted in a 10-fold greater sensitivity than for a coating applied to the rim of the electrode. Consequently, the total surface was coated with the conducting salt as uniformly as possible in the experiments described below. Attempts to prepare films by solvent-casting techniques using acetonitrile or acetone solutions of the 9-$AA^+(TCNQ)_2^-$ compound were not successful.

Results and Discussion

Cyclic Voltammetry/EQCM. To activate the TCNQ redox couple, oxidation of a newly prepared (9-aminoacridinium$^+$)$(TCNQ)_2^-$ surface film was performed in the 0.4 to 0.6 V (vs. S.C.E.) region. EQCM of this activation process was briefly examined, but was not the main focus of the present study. Typical behavior is shown in Figure 1, which depicts six segments of a cyclic voltammogram obtained on a (9-aminoacridinium$^+$)$(TCNQ)_2^-$ electrode in 1 M $Ca(OAc)_2$. Values of Δfreq and ΔQ for the redox transitions are given in Table 1.

The activation process, which in this case was performed by application of the initial potential at 0.6 V, resulted in a small increase in the frequency and a corresponding anodic transient. This step is denoted by Ox1 in Figure 1; subsequent redox steps in a sweep segment are denoted as R1, Ox2, R2 (—). In the experiment of Figure 1, the

(9) Hillman, A. R.; Swann, M. J.; Bruckenstein, S. *J. Phys. Chem.* **1991**, *95*, 3271–3277. Hillman, A. R.; Loveday, D. C.; Bruckenstein, S. *J. Electroanal. Chem.* **1991**, *300*, 67.
(10) Bruckenstein, S.; Wilde, C. P.; Hillman, A. R. *J. Phys. Chem.* **1993**, *97*, 6853 and papers cited therein.
(11) Mounts, R. D.; Widlund, K.; Gunadi, H.; Perez, J.; Pech, B.; Chambers, J. Q. *J. Electroanal. Chem.* **1992**, *340*, 227–239.
(12) Boyd, R. H.; Phillips, W. D. *J. Chem. Phys.* **1965**, *43*, 2927.
(13) Sharp, M. *Anal. Chim. Acta* **1976**, *85*, 17. Sharp, M.; Johansson, G. *Ibid.* **1971**, *54*, 13.
(14) Inzelt, G.; Day, R. W.; Kinstle, J. F.; Chambers, J. Q. *J. Phys. Chem.* **1983**, *87*, 4592.
(15) Hillier, A. C.; Ward, M. D. *Anal. Chem.* **1992**, *64*, 2539–2554.
(16) Bacskai, J.; Lang, G.; Inzelt, G. *J. Electroanal. Chem.* **1991**, *319*, 55–69.

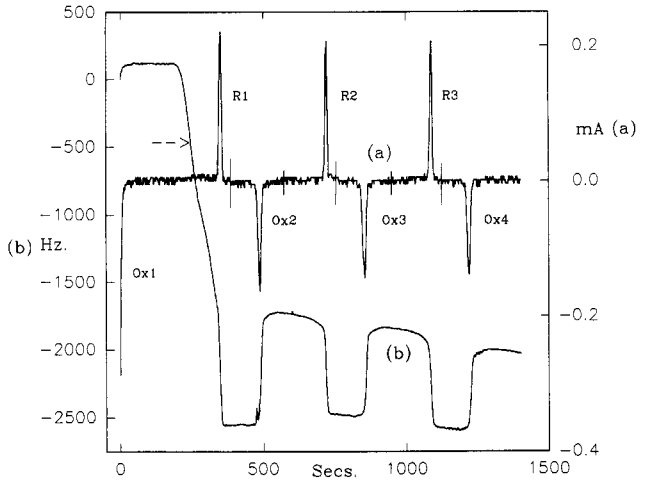

Figure 1. (a) Cyclic voltammogram, (b) QCM frequency response of 9-AA,$TCNQ_2$ film in 1 M $Ca(OAc)_2$; sweep rate 2 mV s^{-1}; potential range 600 to −100 mV followed by cycling between −100 and 300 mV; the switching potentials are marked by vertical lines on the current axis.

Table 1. EQCM of 9-Aminoacridinium TCNQ Electrodes

1 M $Ca(OAc)_2$[a]	freq (Hz)	Q (mC)	eq mass (g/equiv)
Ox1			
R1	2685	2.39	361
Ox2	834	2.45	110
R2	759	2.30	106
Ox3	650	2.20	95
R3	748	2.13	112
Ox4	575	2.11	88
1 M KOAc[b]	**freq (Hz)**	**Q (mC)**	**eq mass (g/equiv)**
Ox1			
R1	1333	0.887	482
Ox2		0.704	
R2	393	0.713	177
Ox3	184	0.702	84
R3	241	0.657	117
Ox4	192	0.599	102
R1′	448	1.36	106
Ox1′	77	1.08	23
R2′	282	0.873	104
Ox2′	205	0.809	81
R3′	231	0.754	98
Ox3′	205	0.708	93
R4′	251	0.679	119
Ox4′	212	0.626	108

[a] Sweep rate 2 mV/s; sweep limits 600 to −100 mV to 300 mV. [b] Sweep rate 10 mV/s; sweep limits 600 to −100 to 350 mV.

small frequency increase is consistent with loss of a proton as suggested previously. However, this behavior was not always seen. In the presence of bromide electrolytes, frequency decreases were seen when the potential was swept into the 0.4–0.6-V region for a newly prepared electrode surface. We suspect that the frequency decreases seen in the activation step were due to anion ingress into, or anion adsorption onto, the surface film structure. This idea is presented in greater detail below for the subsequent oxidation steps: Ox2, Ox3 (—).

Further examination of the cyclic EQCM data reveals several subtle features of the surface redox processes that are not seen in either the cyclic voltammogram or the spectroelectrochemical results. The previous study[11] established that the redox waves produced by the initial activation (see Figure 2) involve a neutral/dimer dianion TCNQ couple:

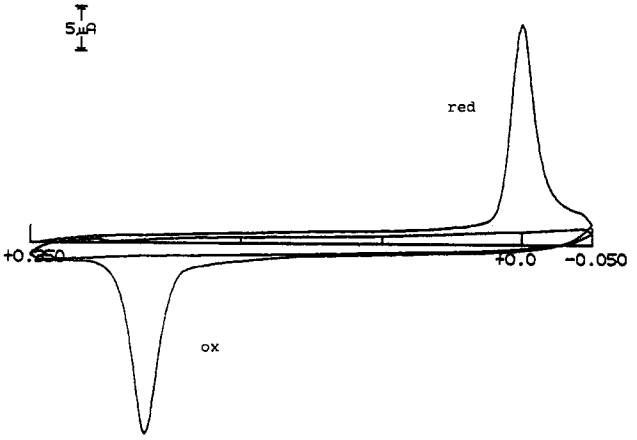

Figure 2. Cyclic voltammogram of TCNQ couple generated from a 9-AA,$TCNQ_2$ film in 1.0 M $Ca(OAc)_2$ on a glassy carbon electrode; sweep rate 10 mV s^{-1}.

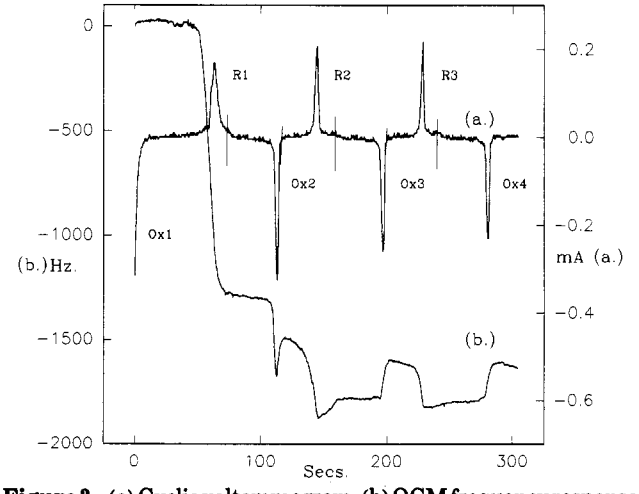

Figure 3. (a) Cyclic voltammogram, (b) QCM frequency response of 9-AA,$TCNQ_2$ film in 1 M KOAc; sweep rate 10 mV s^{-1}; potential range 600 to −100 mV followed by cycling between −100 and 350 mV; the switching potentials are marked by vertical lines on the current axis.

$$TCNQ,TCNQ + 2M^+ + 2e^- \rightleftharpoons (TCNQ)_2^{2-}(M^+)_2 \quad (2)$$

The well-defined isosbestic points that were seen indicated that only two redox states exist in the films, even though the redox processes are separated by ca. 0.24 V. However, the EQCM data invariably indicated that the mass (and/or viscosity) increase due to the first reduction process (R1) following the activation was considerably larger than the subsequent changes. Another persistent feature of the EQCM data was that frequency changes were seen in the potential regions where there was no obvious faradaic current in the voltammograms. These frequency changes had time constants much slower than expected for simple nonfaradaic adsorption phenomena. In Figure 1 these "prewave mass changes" are most evident for the reduction steps. However, they were often observed as well for the oxidation steps. These prewave mass changes, which were evident even at slow sweep rates, indicate nonequilibrium kinetically controlled behavior. This is supported by the potential step EQCM experiments described below.

Several cycles between the oxidized and reduced states were required in order to establish both a chemically reversible voltammetric and EQCM response. This behavior is shown in Figures 3 and 4 for the TCNQ salt electrode in contact with 1 M KOAc. While the Ox1 and

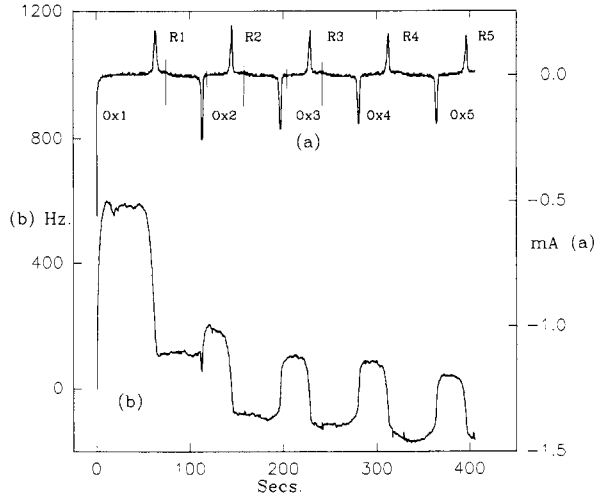

Figure 4. (a) Cyclic voltammogram, (b) QCM frequency response of 9-AA,$TCNQ_2$ film in 1 M KOAc; reactivation and recycling of the film of Figure 2; same experimental conditions.

R1 EQCM response is similar to that of Figure 1, the Ox2 transition indicates a mass increase followed by a slow mass loss. Several redox cycles were required before the square-wave ion motion pattern was developed for this electrode. Figure 4 shows this pattern for the same electrode after it had been allowed to come to equilibrium at open circuit in a reduced state.

Once an electrode was cycled several times, the approximate equivalent mass values for the redox transitions became reproducible even though the total charge decreased with each cycle. (It was found that the TCNQ couple was much less persistent on the gold contacts of the quartz crystals than on glassy carbon electrodes.) While there are uncertainties in the calculation as described above, the values of the equivalent mass for the redox transitions are of interest and are given in Table 1. With the exclusion of the first or secnd transitions, the values are 102 ± 10 and 100 ± 13 g/equiv for the $Ca(OAc)_2$ and KOAc electrolyte solutions, respectively.

A comment on the significance of the equivalent mass values is appropriate. These values are consistent with cathodic insertion of $CaOAc^+$ (molar mass = 99) and $K(H_2O)_4^+$ (molar mass = 111) ions into the electrode lattice structure. (Based on literature formation constants, the $CaOAc^+$ species is the principal species in 1 M $Ca(OAc)_2$ solution.[17]) In view of the uncertainties with regard to the viscoelastic and morphological changes that must take place upon redox cycling of the TCNQ electrode, however, definite assignment of the mass transitions to these species cannot be made. The equivalent mass values calculated from Δf values obtained on relatively thin films, where surface morphology effects are expected to be more significant, tended to be larger than the above values.

It is informative to analyze the EQCM data following the treatment of Hillman and Bruckenstein.[9] They introduced a function Φ which is a linear combination of the mass change, ΔM, and the equivalent mass derived from the faradaic charge:

$$\Phi_j = \Delta M + Q(m_j/z_jF) \quad (3)$$

In eq 3 the subscript j refers to a particular ion with mass

(17) *Lange's Handbook of Chemistry*, 13th ed.; Dean, J. A., Ed.; McGraw-Hill: New York, 1985; pp 5–77.

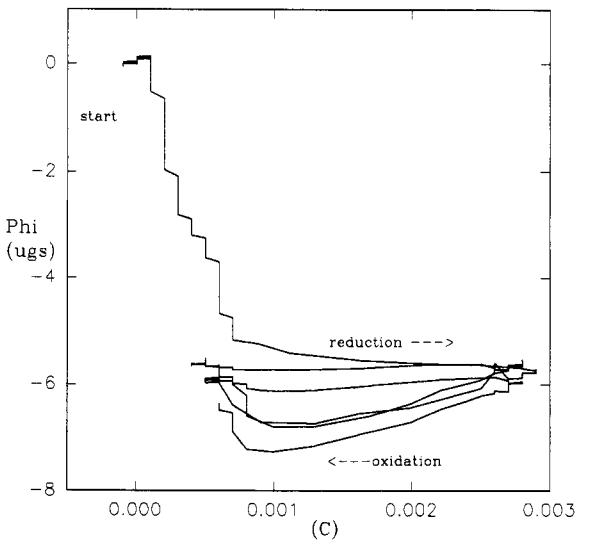

Figure 5. Plot of Φ_{CaOAc^+} vs Q for data in Figure 1; sweep rate 2 mV s^{-1}; arrows indicate direction of potential sweep.

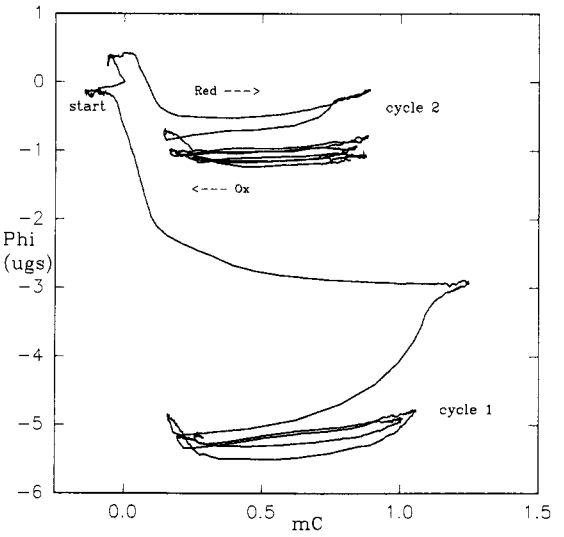

Figure 6. Plot of $\Phi_{K(H_2O)_4^+}$ vs Q for data in Figure 2 represented in cycle 1 and data in Figure 3 represented in cycle 2; sweep rate 10 mV s^{-1}; arrows indicate direction of potential sweep.

m_j and charge z_j. A zero value for Φ_j (or its derivative) indicates that the jth ion is the only mobile species and that the electrode is permselective for that ion.

Figures 5 and 6 show the Hillman and Bruckenstein Φ plots for the principal cations in the $Ca(OAc)_2$ and KOAc electrolyte solutions. In the former case, the mass of the $CaOAc^+$ ion was used, and the latter, the mass of the $K(H_2O)_4^+$ ion was used. After the initial reduction step (R1), the values of Φ tend to become invariant with the charge passed in the slow sweep cyclic voltammograms. This indicates that these cations are responsible for the square wave ion motion pattern seen in Figures 3 and 4.

The values of the frequency changes following R1 relative to the change for R2 indicate that considerable solvation of the conducting salt film has occurred during the initial reduction step. Thus in the first reduction step ingress of $M^+(H_2O)_n$ is coupled to the charge transport, where M^+ is the predominant cation in the electrolyte solution, either K^+ or $Ca(OAc)^+$ for Figures 1 and 3. The plots show that after the initial excursions of the Φ functions during the R1 and Ox2 transitions, the values become invariant with Q. This indicates that the con-

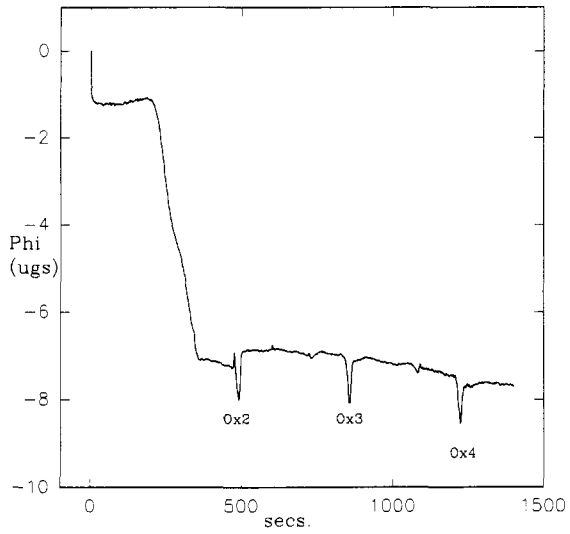

Figure 7. Plot of Φ_{CaOAc^+} vs time for the experiment of Figure 1.

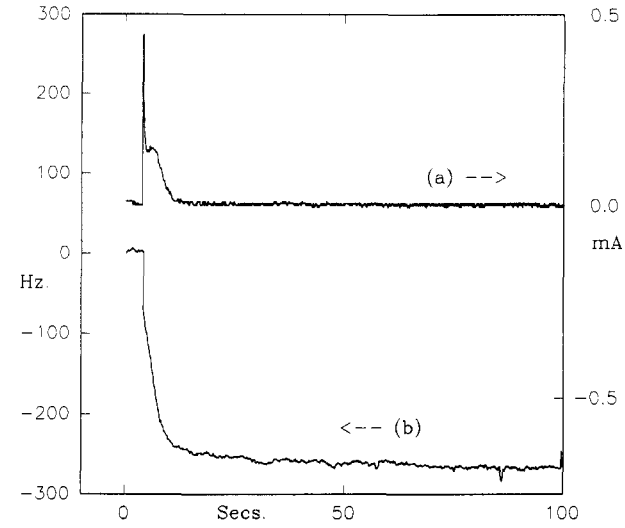

Figure 8. (a) Current and (b) frequency response for a 9-AA,$TCNQ_2$ film stepped to -31 mV in 1 M $Ca(OAc)_2$.

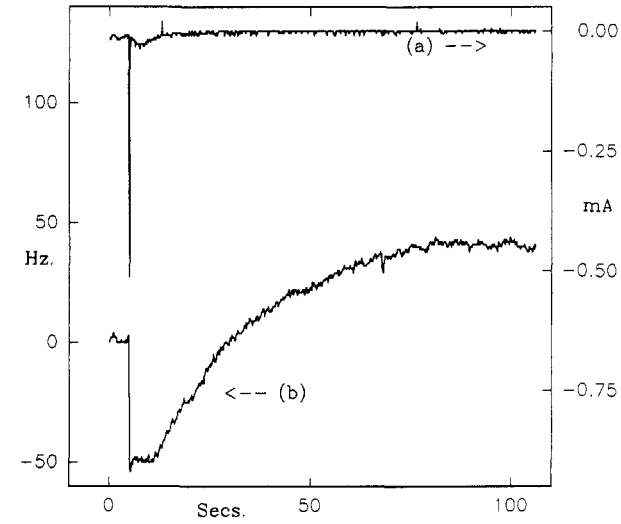

Figure 9. (a) Current and (b) frequency response for a 9-AA,$TCNQ_2$ film stepped to 145 mV in 1 M $Ca(OAc)_2$.

ducting salt films have become permselective with respect to the predominant cation in the solution.

Careful inspection of the Φ vs Q plots reveals that permselectivity is more rigorously obeyed during the cathodic transients than during the anodic transients. This is indicated by the curvature seen in these plots during the anodic transients. A more dramatic representation of this phenomenon is provided by Figure 7 in which the Φ_{CaOAc^+} data derived from Figure 1 have been plotted on the same time scale as Figure 1. This effect is discussed in more detail below in conjunction with the chronoamperometric results.

Another feature of the EQCM results is that the mass transition for the first reduction step after initial activation was much greater than the subsequent Ox/R steps. (This is marked by an arrow in Figure 1.) These excursions indicate uptake of neutral solvent and/or supporting electrolyte species. However, surface morphological differences are likely to exist between the initial and redox cycled states which result in viscoelastic differences that contribute to the observed behavior. These changes are probably related to the structural changes that are required to accommodate the ingress of the ions of the supporting electrolyte into the lattice of the conducting salt.

Chronoamperometry/EQCM. Potential step experiments were carried out on TCNQ salt electrodes in concentrated potassium and calcium electrolyte solutions. Both the current and the frequency trnasients indicated additional complexity to the electrode processes. It should be noted that the electrodes in these experiments were activated in the usual manner and cycled several times before performing the potential steps. Before each step, the electrode was held at an appropriate potential to fully oxidize or reduce the surface film.

Figure 8 shows the cathodic EQCM transient behavior for a TCNQ salt electrode in 1 M $Ca(OAc)_2$ when the potential was stepped into the rising segment of the surface peak voltammogram. At low overpotentials, the current response exhibited a clear two-step behavior that consisted of a fast component, which was completed in 1–2 s and a slow component for which the time scale varied with the applied potential. The frequency response of the QCM, however, showed a monotonic decrease that took place roughly on the time scale of the two components of the current transient. In experiments on glassy carbon substrates (not shown) it was demonstrated that applied potentials on the foot of the voltammetric waves were sufficient to completely switch the surface film between redox states. Thus for the EQCM experiments, it is reasonable to conclude that the films are fully redox switched at potentials on the feet of the voltammetric waves.

The two-step behavior of the current transient was also seen on the anodic side when the potential was stepped into the foot of the oxidation wave. It is speculated that the faster response is due to redox reactions of lattice sites that are readily accessible by counter ions and that the slower response is due to sites with restricted access for solution cations. In this view the TCNQ salt electrode has features of a porous electrode, a picture consistent with the extensive hydration of the electrode that takes place upon initial activation of the surface.

The anodic frequency/mass transients exhibited an additional feature. Typical behavior is shown in Figure 9 for a step to the midpoint of the oxidation wave. There was an initial rapid apparent mass increase coincident with the application of the potential, which was then followed by a slow frequency increase on a time scale much longer than the current transient. This behavior indicates

that prior to expulsion of the cation in the oxidation step, there is uptake of anions from the electrolyte solution. Equation 4 presents a qualitative explanation of this behavior.

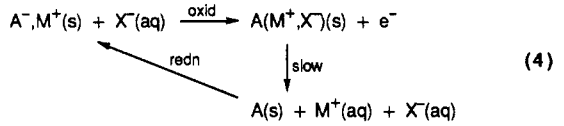

(4)

In this equation A represents the TCNQ acceptor site and M^+,X^- is the electrolyte, $CaOAc^+,OAc^-$ in this case. The slow frequency/mass transient in this view is due to loss of the neutral salt from the electrode/solution interface. Entirely similar behavior was seen by Haas and co-workers for ion motion at a phenazine redox polymer electrode.[18] It can be mentioned that this qualitative behavior was often seen in the numerous EQCM/CV experiments that were performed in the course of this investigation; i.e., upon initial redox cycling anodic frequency transients were seen that had an initial negative component followed by a slower positive excursion that took place in the apparent absence of faradaic current. This mechanism also explains the excursions of the Φ values seen during the anodic steps in Figure 7.

These slow mass transients are easily rationalized qualitatively in terms of the above scheme. To maintain charge neutrality, migrational motion of the ions is required. Since migration of electrostatically bound M^+ ions from the M^+,A^- surface/lattice states should be slower than migration of free $X^-(aq)$ ions from the concentrated electrolyte solution, formation of "occluded" electrolyte is expected.

Analysis of the Chronoamperometric Mass Transients. The slow mass transients observed upon stepping the potential to positive values in the foot of the anodic wave are indicative of a Fickian diffusion process. Negligible faradaic current was observed during these transients. The process can be modeled by diffusive dissipation of a plug of material from a channel of depth, d, at the electrode solution interface. Following eq 4 above, the diffusing material is the salt M^+,X^- from the surface of the conducting salt electrode. For linear diffusion in an uniform film, this process can be described by eq 5,[19] where

$$C = (C^*/2)\{\mathrm{erf}[(d-x)/2\sqrt{Dt}] + \mathrm{erf}[(d+x)/2\sqrt{Dt}]\} \quad (5)$$

C is the concentration of the salt as a function of time and distance, C^* is the initial concentration of the salt in the pore (after application of the potential and before dissolution of the salt commences), and D is a diffusion coefficient. Integration of this equation between $x = 0$ and $x = d$ gives the film surface coverage (Γ) as a function of time.

The integration was performed graphically using the figure in Carslaw and Jaeger.[19] Inspection revealed that the plot of Γ vs $t^{1/2}$ was linear as $t \rightarrow 0$ in a Cottrellian

$$\Gamma/\Gamma^* = (0.987 \pm 0.0046) - (0.5533 \pm 0.0129)\sqrt{(Dt)}/d \quad (6)$$

fashion. The linear least-squares fit was given by eq 6, with $r = 0.9986$ for the seven points with $Dt/d^2 < 0.5$. This corresponds to a slope of 1.78^{-1} or approximately $\pi^{1/2}$. The slope is thus given by eq 7, where τ is a characteristic time

$$(d\Gamma/d\sqrt{t})_{t\rightarrow 0} = \Gamma^*(D/\pi)^{1/2}/d = \Gamma^*/\pi^{1/2}\tau^{1/2} \quad (7)$$

constant. Crank gives a very similar result, which differs from eq 7 only in the constant, for slightly different boundary conditions.[20]

Despite the nonuniform nature of the films, qualitative agreement with this model was found in that the plots of frequency vs $t^{1/2}$ displayed linear segments at short times that allowed time constants for the apparent diffusion process to be evaluated. Data are collected in Table 2. The Γ^* values necessary to calculate the time constants given in Table 2 were estimated from the respective frequency vs time data for the individual electrodes. In Table 2, τ values and not D values are given since the film thicknesses necessary to calculate the latter were not generally known (or meaningful for a nonuniform film).

The diffusion time constants of Table 2 were found to be potential and anion dependent as shown in Figure 10. In particular, for the acetate electrolytes, the diffusional loss of the electrolyte from the fully oxidized surface is faster than from the partially oxidized surface by several orders of magnitude. This can also be qualitatively understood in terms of the above model since fully oxidized ion channels would not have any residual M^+,A^- sites to impede loss of neutral electrolyte either by electrostatic attraction or by blocking of the ion channels.

Table 2. EQCM Chronoamperometry on 9-AA^+,$TCNQ_2^-$ Film Electrodes

electrolyte	E (mV vs SCE)	slope (μg s$^{-1/2}$)	C^* (μg)	log(τ/s)
1.0 M KBr	240	0.051	0.6	1.6
	260	0.062	1.1	2.0
	250	0.13	1.2	1.4
	250	0.15	1.2	1.3
	240	0.044	0.6	1.8
	260	0.064	1.0	1.9
1.0 M KOAc	260	0.55	1.5	0.4
	240	0.28	1.3	0.8
	260	0.32	1.0	0.5
	290	0.78	1.2	−0.1
1.0 M $Ca(OAc)_2$	110	0.012	0.8	3.1
	120	0.010	1.2	3.7
	145	0.058	0.35	1.1
	154	0.086	0.20	0.2

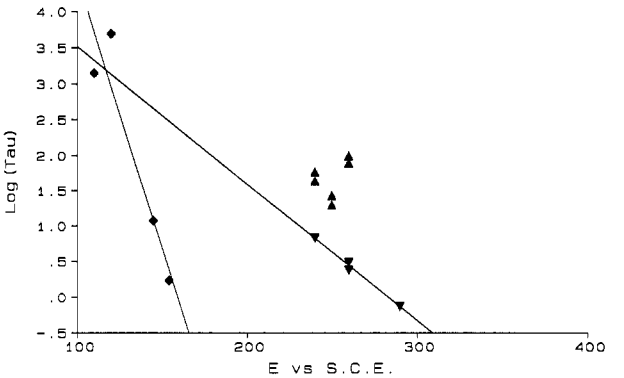

Figure 10. Potential dependence of diffusional time constants calculated from the anodic frequency transients: (◆) 1.0 M $Ca(OAc)_2$, (▼) 1.0 M KOAc, (▲) 1.0 M KBr. Least-squares lines have been drawn through the $Ca(OAc)_2$ and KOAc data with slopes of 52 ± 4 and 13 ± 3 mV^{-1}, respectively.

(18) Miras, M. C.; Barbero, C.; Kötz, R.; Haas, O.; Schmidt, V. M. *J. Electroanal. Chem.* **1992**, *338*, 279.

(19) Carslaw, H. S.; Jaeger, J. C. *Conduction of Heat in Solids*, 2nd ed.; Oxford University Press: London, 1959; p 55.

(20) Crank, J. D. *Mathematics of Diffusion*; Clarendon Press: Oxford, 1975.

Conclusions

These EQCM experiments have provided considerable additional information regarding the nature of the TCNQ surface redox reactions in the 9-aminoacridinium–TCNQ system. First of all, the mass transients indicate cathodic insertion of cations into the solid-state lattice and, at slow sweep rates, expulsion of the cations in the anodic process. The magnitude of the mass changes are consistent with $K(H_2O)_4^+$ and $CaOAc^+$ as the mobile species in these reactions. After redox cycling, permselective ion motion is observed for these species in concentrated KBr and $Ca(OAc)_2$ aqueous solutions.

The initial reduction step after activation of the surface gave anomalously large mass transients indicative of extensive hydration or surface structural change. In the latter situation, surface roughness or solvent trapped in ion channels would contribute to the frequency decrease of the quartz crystal.

Especially interesting were the very slow mass transients seen in the anodic chronoamperometric experiments. These are consistent with the scheme embodied in eq 4: insertion of anions of the supporting electrolyte in order to maintain charge neutrality, followed by the slow diffusional loss of neutral electrolyte. This process gave rise to significant frequency transients in the cyclic voltammetry EQCM experiment at potentials where there was essentially no faradaic reaction taking place. In contrast to the anodic reaction, the cathodic mass transients were indicative of direct incorporation of the cation of the electrolyte into the solid-state lattice.

The slow anodic frequency transients were modeled by Fickian diffusion from an ion channel of finite depth. The diffusive time constants were electrolyte dependent. Further work is in progress to understand the nature of this phenomenon.

Acknowledgment. This work was supported by a grant from the National Science Foundation (CHE-9220939) and by the University of Tennessee. Dr. Richard Mounts is thanked for his comments and for a sample of the TCNQ salt used in our initial studies.